JACS
JOURNAL OF THE AMERICAN CHEMICAL SOCIETY

Communication

pubs.acs.org/JACS

Superprotonic Conductivity in a Highly Oriented Crystalline Metal–Organic Framework Nanofilm

Gang Xu,[†] Kazuya Otsubo,[†,‡] Teppei Yamada,[†] Shun Sakaida,[†] and Hiroshi Kitagawa*[,†,‡,⊥,§]

[†]Division of Chemistry, Graduate School of Science, Kyoto University, Kitashirakawa Oiwake-cho, Sakyo-ku, Kyoto 606-8502, Japan

[‡]Core Research for Evolutional Science and Technology (CREST), Japan Science and Technology Agency (JST), 7, Gobancho, Chiyoda-ku, Tokyo, 102-0076, Japan

[⊥]Institute for Integrated Cell-Material Sciences (iCeMS), Kyoto University, Yoshida, Sakyo-ku, Kyoto 606-8501, Japan

[§]INAMORI Frontier Research Center, Kyushu University, 744 Motooka, Nishi-ku, Fukuoka 819-3095, Japan

Supporting Information

ABSTRACT: The electrical properties of a highly oriented crystalline MOF nanofilm were studied. This nanofilm has low activation energy and a proton conductivity that is among the highest value reported for MOF materials. The study uncovered the reasons for the excellent performance of this nanofilm and revealed a new pathway for proton transport in MOF materials; besides the channels inside a MOF, the surface of the MOF nanocrystal can also dominate proton transport.

Metal–organic frameworks (MOFs), known as porous coordination polymers, have features such as large surface area, crystalline ordered structure, and highly regularized pores. These materials are potentially useful for gas storage, separations, sensors, catalysis, and drug delivery.[1] While the main effort in this research area is devoted to bulky MOFs (single crystals, polycrystalline powders, etc.),[2] many electrical, magnetic, and optical applications require the use of the thin film form of MOF materials.[3] At present, studies of MOF nanofilms are rare; the preparation of highly oriented crystalline MOF nanofilms is difficult, and investigations into the physical properties of MOF thin films are in early infancy.[4]

Proton-conducting materials play a key role in some solid-state electrochemical devices such as batteries and fuel cells.[5] Recently, research into the proton conductivity of MOF materials has aroused much interest, as MOFs offer great potential for the systematic design and modification of proton-conducting properties.[6] Although some of the reported MOF materials have showed high proton conductivity, some questions about proton transport still require answers. For example, besides the channels inside a MOF, can the surface of the MOF crystal act as an efficient pathway for protons? The answer to this question becomes even more critical when the size of the MOF crystal decreases to the nanoscale, because in this situation the outer surface area of nanocrystals increases dramatically. This high external surface area cannot be overlooked when studying the proton-conducting properties of such nanoscale MOF materials.

Here, we report the first study of the electrical properties of a highly oriented and crystalline MOF nanofilm. The MOF nanofilm was fabricated by a "modular assembly" method,[3e] and the proton conductivity of this nanofilm was observed to be among the highest values reported for a MOF material. In this study, the importance of the surface of the MOF nanocrystal to the proton transport is revealed for the first time.

The MOF nanofilm for electrical measurement was constructed by a previously developed "modular assembly" method (Figure 1 and Figures S1 and S2 in Supporting Information [SI]) .[3e] In brief: a MOF (Cu–TCPP) nanosheet with a high aspect ratio (thickness around 15 nm, diameter around 400 nm) was synthesized by the reaction of $Cu(NO_3)_2$ and 5,10,15,20-tetrakis(4-carboxyphenyl)porphyrin (H2TCPP), and then the product was deposited layer by layer onto a preprepared patterned Cr/Au (30/120 nm) electrode on a SiO_2 (300 nm thick)/Si wafer to form the thin film channel between electrodes.

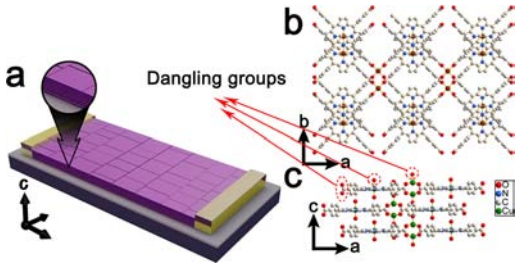

Figure 1. Schematic of the nanosheet-constructed MOF nanofilm for electrical measurement (a) and the modeled crystal structure of the MOF nanofilm (b and c). All H atoms are omitted for clarity.

The Cu–TCPP nanosheet is a two-dimensional (2-D) MOF, where the 2-D reticulation along the *ab* plane is constructed with Cu-centered TCPP units connected by binuclear $Cu_2(COO)_4$ paddle wheels, and 3-D packing is achieved with an AB model along the *c* axis (Figure 1b and c). The Cu–TCPP nanofilm remains crystalline and highly oriented on the substrate. The in-plane patterns of synchrotron grazing-incidence XRD (GIXRD) only shows (*hk*0) peaks, and the out-of-plane patterns show an (00*l*) peak (Figure 2). Therefore, the MOF nanosheets lie with the *ab* plane parallel to the SiO_2/Si substrate.

Received: March 18, 2013
Published: May 7, 2013

   dx.doi.org/10.1021/ja402727d | *J. Am. Chem. Soc.* 2013, 135, 7438–7441

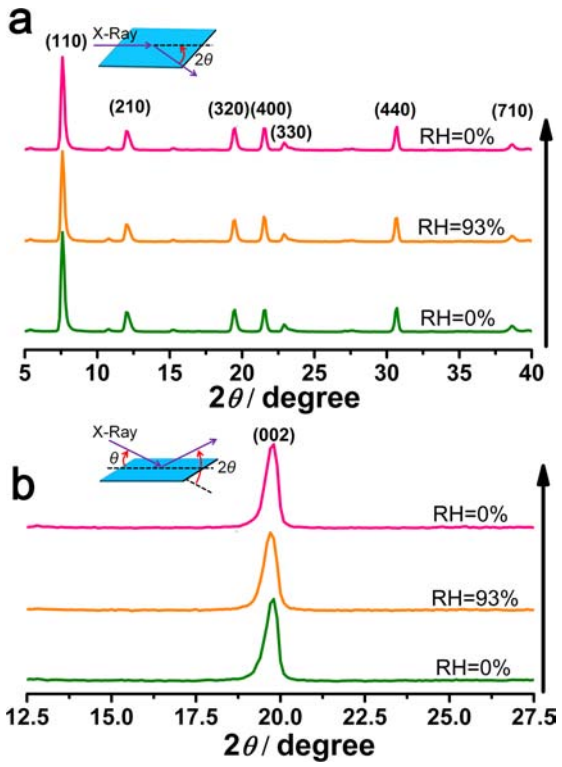

Figure 2. Synchrotron GIXRD (λ = 1.550 Å) of the MOF nanofilm: in-plane patterns (a) and out-of-plane patterns (b). The patterns were measured under RH = 0% for 10 min at first (green), then under RH = 93% for 10 min (yellow), and finally RH = 0% again for 10 min (red).

The Cu−TCPP nanosheet is porous, with a 1-D channel along the *c* axis. From the crystal structure, the diameter of the channel is estimated to be around 1.1 nm (Figure 1b and c).[3e] N_2 gas sorption experiments were performed to examine the surface area and pore volume of the Cu−TCPP nanosheet. The sorption curves are a combination type I/II isotherm (Figure 3)

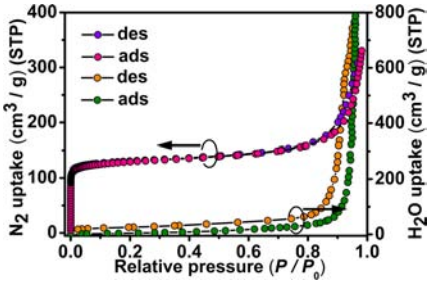

Figure 3. N_2 isotherm (red and purple) and water vapor isotherm (green and yellow) of the Cu−TCPP nanosheet.

with rapid gas uptake at low pressure, indicating the presence of micropores in the nanosheet, followed by gradual N_2 uptake at moderate partial pressures and rapid capillary condensation at high partial pressures, indicating the existence of mesopores. The mesopores probably result from the packing of the nanosheets. The BET surface area was found to be 485 m^2/g for micropores, and total pore volumes were found to be 0.17 cm^3/g for micropores and 0.26 cm^3/g for mesopores at P/P_0 = 0.96.

The preparation of MOF thin films and subsequent study of their electrical properties are desirable because thin film electrolytes are required to fabricate commercial fuel cell devices. For example, a typical Nafion electrolyte membrane in a fuel cell device is in the order of 100 μm thick. The thin film nature reduces the overall resistance of the electrolyte membrane and increases the efficiency of the device.

The electrical properties of the highly oriented MOF nanofilm in this work were determined by depositing the nanofilm between two electrodes, and then performing alternating current (AC) impedance analysis with a quasi-four-probe method (Figure S2 in SI). The proton conductivity was estimated from Nyquist plots (Figures 4b and S3 [SI]).

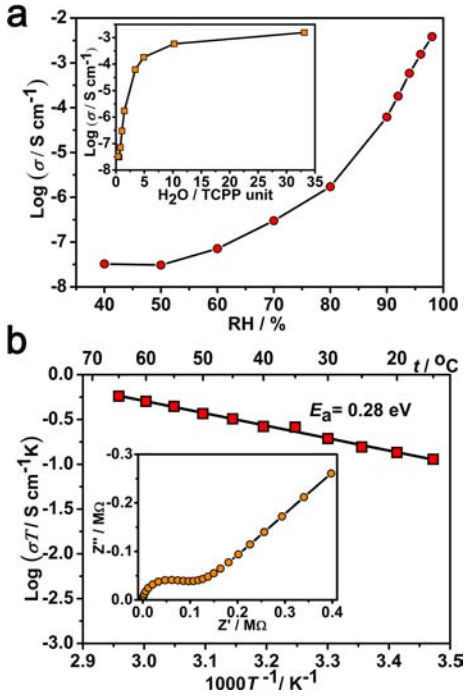

Figure 4. Proton conductivity of the MOF nanofilm under various RH conditions. (a) (Inset) Proton conductivity vs adsorbed water and Arrhenius plots of the proton conductivity of the MOF nanofilm under 95% RH; least-squares fitting is shown as a solid line. (b) (Inset) Typical Nyquist plot of the MOF nanofilm measured under 98% RH at room temperature.

The distance between two electrodes was set to 100 μm, a separation long enough to avoid parasitic currents. The length of the electrode was 3000 μm. The thickness of the MOF thin film was measured to be 350 nm by atomic force microscopy (AFM) (Figure S2 in SI).

The proton conductivity at 25 °C at varying relative humidity (RH) is shown in Figure 4. The nanofilm has a low conductivity of 3.2×10^{-8} S cm^{-1} at 40% RH, which dramatically increases by 3 orders of magnitude to 6.2×10^{-5} S cm^{-1} at 90% RH, and then further increases to 3.9×10^{-3} S cm^{-1} at 98% RH. It is important to note that the value of 3.9×10^{-3} S cm^{-1} at 98% RH reported here is not only the highest value yet recorded for a hydrated MOF sample but is also comparable to the proton conductivity of an acid-impregnated MOF material.[7]

To further investigate the unusually high conductivity of the MOF nanofilm, in situ synchrotron GIXRD of the thin film under varying RH conditions and water sorption experiments of the Cu−TCPP nanosheet were performed. As shown in Figure 2, the GIXRD patterns (in-plane and out-of-plane) of

dx.doi.org/10.1021/ja402727d | J. Am. Chem. Soc. 2013, 135, 7438−7441

the nanofilm show almost no difference under varying RH conditions, demonstrating that the nanofilm remains intact at high humidity. The constant GIXRD patterns with varying RH also exclude the "gate-opening" effect in this 2-D MOF under high humidity.

The water sorption curves (Figure 3) are similar to a type-V isotherm and only 76 cm^3 (STP) water was adsorbed by 1 g nanosheet (4 H_2O/TCPP unit) before P/P_0 = 0.9, which demonstrates very weak interaction between adsorbate and adsorbent, as well as the hydrophobic nature of the adsorbent. However, after P/P_0 = 0.9, rapid capillary condensation occurs, up to a value of 780 cm^3/g (STP) (34 H_2O/TCPP unit), and a significant hysteresis is observed. For a hydrophobic MOF material that lacks a large number of highly favorable adsorption sites (e.g., cations, open-metal sites), the water condensation would be caused by the overlapping potential of the pore walls and would be controlled by the size of the pore—the smaller the size of the pore the lower the P/P_0 for water condensation.[8] Therefore, for the Cu−TCPP nanosheet, where the size of the micropores is around 1.1 nm, the pore filling should normally occur before P/P_0 = 0.5. The fact that the pore filling takes place after P/P_0 = 0.8 (Figure 3) clearly indicates that water adsorption does not take place in the micropores inside the nanosheet but in the mesopores or macropores among the nanosheets.[7] Considering that the proton conductivity strongly depends on RH and water is adsorbed in the mesopores or macropores among the nanosheets, we may deduce that the hydrogen-bonding network which acts as the pathway for proton transport is created by adsorbed water, dangling coordination water, and dangling carboxyl groups of the nanosheet (Figure 1c), and therefore it should locate within the mesopores or macropores and/or on the surface of the nanosheet.

This hypothesis could be further clarified by analyzing the conductivity (Log σ) versus adsorbed water/TCPP unit. As shown in Figure 4a inset and Figure S4 [SI], when RH increases from 40% to 90%, 4 mol water is adsorbed by 1 mol TCPP unit, resulting in an increase in conductivity by 3.5 orders of magnitude. At this stage, the water molecule is only adsorbed on the surface of the nanosheet, far from the multilayer adsorption or condensation at 96% RH. In the RH range from 90% to 96%, the uptake of water suddenly increases to 34 H_2O/TCPP unit. At this high uptake, the conductivity trends to saturation (Figure 4a inset), and the value of the conductivity increases slightly by about 1 order of magnitude.

The above analysis clearly indicates that the small amount of water adsorbed before 90% RH can already create an efficient pathway on the surface of the nanosheet for proton transport, exerting control over most of the change in the proton conductivity. Hence, the surface of the Cu−TCPP nanosheet, which contains numerous dangling groups (Figure 1c), should play the dominant role in constructing the proton pathway.

The unusually high conductivity of our MOF thin film may arise from the numerous dangling groups on the surface of the nanosheet and the highly oriented crystalline morphology of the thin film. The size effect of the nanosheets used to build the thin film should also be noted. The dimensions of the Cu−TCPP crystal are within the nanoscale; hence, there are numerous groups on the surface of the nanosheet, such as acidic coordinated waters on the Cu atom, and noncoordinated carboxyl groups (Figure 1c). These dangling groups can act as Lewis acids. They have been reported to be effective proton donors and can be utilized to design MOF materials with high proton conductivity.[5,6,9] On the other hand, the GIXRD (Figure 2) has demonstrated that the thin film is fabricated by aligning Cu−TCPP nanosheets in a highly oriented way. It has been proved that unidirectional growth or highly oriented packing of crystals can improve the performance of electrolytes.[10]

The temperature-dependent proton conductivities of the MOF nanofilm at RH 95% were measured, as shown in Figure 4b. The activation energy of proton conductivity was calculated to be 0.28 eV from the least-squares fits of the slopes. This value is quite small and comparable to that of Nafion (E_a = 0.22 eV), a high conducting material used in commercial fuel cells. Hence, similar to the case of Nafion, the mechanism of proton conductivity should be assigned to the Grotthuss mechanism (E_a = 0.1−0.4 eV), not the vehicle mechanism (E_a = 0.5−0.9 eV).

In conclusion, the electrical properties of a MOF nanofilm were studied for the first time. Results indicated that the proton conductivity of this nanofilm is not only the highest value for a hydrated MOF sample, but it is also comparable to that of an acid-impregnated MOF material. We propose that this remarkable proton conductivity may originate from the highly oriented packing of the nanosheet along with numerous dangling functional groups on the surface of the nanosheet. Our research suggests the importance of the surface of the MOF crystal to proton transport. These effects are especially important when the size of the MOF crystal decreases to the nanoscale, where the surface of the nanocrystal can play a dominant role in proton conductivity. Our work would benefit the utilization of MOF material in micropower systems, such as microfuel cells and microbatteries.

■ ASSOCIATED CONTENT

Supporting Information

Experimental details, optical microscopy image, AFM image, Nyquist plots, temperature-dependent powder X-ray diffraction patterns, and thermogravimetric analysis curve. This material is available free of charge via the Internet at http://pubs.acs.org.

■ AUTHOR INFORMATION

Corresponding Author

kitagawa@kuchem.kyoto-u.ac.jp

Notes

The authors declare no competing financial interests.

■ ACKNOWLEDGMENTS

This work was partly supported by Grants-in-Aid for Scientific Research No. 20350030 and No. 23245012 from the Ministry of Education, Culture, Sports, Science and Technology of Japan. G. X. thanks JSPS for a postdoctoral fellowship, No. P11339. Synchrotron XRD measurements were supported by the Japan Synchrotron Radiation Research Institute (JASRI) (Proposal No. 2012B1304, No. 2012B1570).

■ REFERENCES

(1) (a) Chae, H. K.; Siberio-Perez, D. Y.; Kim, J.; Go, Y.; Eddaoudi, M.; Matzger, A. J.; O'Keeffe, M.; Yaghi, O. M. *Nature* **2004**, *427*, 523. (b) Farha, O. K.; Shultz, A. M.; Sarjeant, A. A.; Nguyen, A. T.; Hupp, J. T. *J. Am. Chem. Soc.* **2011**, *133*, 5652. (c) Murray, L. J.; Dinca, M.; Long, J. R. *Chem. Soc. Rev.* **2009**, *38*, 1294. (d) Li, J. R.; Sculley, J.; Zhou, H. C. *Chem. Rev.* **2012**, *112*, 869. (e) Shimomura, S.; Higuchi, M.; Matsuda, R.; Yoneda, K.; Hijikata, Y.; Kubota, Y.; Mita, Y.; Kim, J.; Takata, M.; Kitagawa, S. *Nat. Chem.* **2010**, *2*, 633. (f) Sumida, K.;

Rogow, D. L.; Mason, J. A.; McDonald, T. M.; Bloch, E. D.; Herm, Z. R.; Bae, T. H.; Long, J. R. *Chem. Rev.* **2012**, *112*, 724. (g) Férey, G.; Mellot-Draznieks, C.; Serre, C.; Millange, F.; Dutour, J.; Surble, S.; Margiolaki, I. *Science* **2005**, *309*, 2040. (h) Hurd, J. A.; Vaidhyanathan, R.; Thangadurai, V.; Ratcliffe, C. I.; Moudrakovski, I. L.; Shimizu, G. K. H. *Nat. Chem.* **2009**, *1*, 705. (i) Kurmoo, M. *Chem. Soc. Rev.* **2009**, *38*, 1353. (j) Wang, M. S.; Guo, S. P.; Li, Y.; Cai, L. Z.; Zou, J. P.; Xu, G.; Zhou, W. W.; Zheng, F. K.; Guo, G. C. *J. Am. Chem. Soc.* **2009**, *131*, 13572.

(2) (a) Yaghi, O. M.; O'Keeffe, M.; Ockwig, N. W.; Chae, H. K.; Eddaoudi, M.; Kim, J. *Nature* **2003**, *423*, 705. (b) Férey, G. *Chem. Soc. Rev.* **2008**, *37*, 191. (c) Seo, J. S.; Whang, D.; Lee, H.; Jun, S. I.; Oh, J.; Jeon, Y. J.; Kim, K. *Nature* **2000**, *404*, 982. (d) Kitagawa, S.; Kitaura, R.; Noro, S. *Angew. Chem., Int. Ed.* **2004**, *43*, 2334. (e) Southon, P. D.; Price, D. J.; Nielsen, P. K.; McKenzie, C. J.; Kepert, C. J. *J. Am. Chem. Soc.* **2011**, *133*, 10885. (f) Neville, S. M.; Halder, G. J.; Chapman, K. W.; Duriska, M. B.; Moubaraki, B.; Murray, K. S.; Kepert, C. J. *J. Am. Chem. Soc.* **2009**, *131*, 12106.

(3) (a) Makiura, R.; Motoyama, S.; Umemura, Y.; Yamanaka, H.; Sakata, O.; Kitagawa, H. *Nat. Mater.* **2010**, *9*, 565. (b) Makiura, R.; Kitagawa, H. *Eur. J. Inorg. Chem.* **2010**, *2010*, 3715. (c) Motoyama, S.; Makiura, R.; Sakata, O.; Kitagawa, H. *J. Am. Chem. Soc.* **2011**, *133*, 5640. (d) Otsubo, K.; Haraguchi, T.; Sakata, O.; Fujiwara, A.; Kitagawa, H. *J. Am. Chem. Soc.* **2012**, *134*, 9605. (e) Xu, G.; Yamada, T.; Otsubo, K.; Sakaida, S.; Kitagawa, H. *J. Am. Chem. Soc.* **2012**, *134*, 16524.

(4) (a) Bétard, A.; Fischer, R. A. *Chem. Rev.* **2012**, *112*, 1055. (b) Shekhah, O.; Liu, J.; Fischer, R. A.; Wöll, C. *Chem. Soc. Rev.* **2011**, *40*, 1081. (c) Zacher, D.; Shekhah, O.; Wöll, C.; Fischer, R. A. *Chem. Soc. Rev.* **2009**, *8*, 1418. (d) Tsotsalas, M.; Umemura, A.; Kim, F.; Sakata, Y.; Reboul, J.; Kitagawa, S.; Furukawa, S. *J. Mater. Chem.* **2012**, *22*, 10159. (e) Biemmi, E.; Scherb, C.; Bein, T. *J. Am. Chem. Soc.* **2007**, *129*, 8054. (f) Guo, H.; Zhu, G.; Hewitt, I. J.; Qiu, S. *J. Am. Chem. Soc.* **2009**, *131*, 1646. (g) Ameloot, R.; Stappers, L.; Fransaer, J.; Alaerts, L.; Sels, B. F.; De Vos, D. E. *Chem. Mater.* **2009**, *21*, 2580. (h) Allendorf, M. D.; Houk, R. J. T.; Andruszkiewicz, L.; Talin, A. A.; Pikarsky, J.; Choudhury, A.; Gall, K. A.; Hesketh, P. J. *J. Am. Chem. Soc.* **2008**, *130*, 14404. (i) Kreno, L. E.; Hupp, J. T.; Van Duyne, R. P. *Anal. Chem.* **2010**, *82*, 8042. (j) Ameloot, R.; Gobechiya, E.; Uji-i, H.; Martens, J. A.; Hofkens, J.; Alaerts, L.; Sels, B. F.; De Vos, D. E. *Adv. Mater.* **2010**, *22*, 2685. (k) Carbonell, C.; Imaz, I.; Maspoch, D. *J. Am. Chem. Soc.* **2011**, *133*, 2144. (l) Zhuang, J.-L.; Ceglarek, D.; Pethuraj, S.; Terfort, A. *Adv. Funct. Mater.* **2011**, *21*, 1442. (m) Falcaro, P.; Hill, A. J.; Nairn, K. M.; Jasieniak, J.; Mardel, J. I.; Bastow, T. J.; Mayo, S. C.; Gimona, M.; Gomez, D.; Whitfield, H. J.; Riccò, R.; Patelli, A.; Marmiroli, B.; Amenitsch, H.; Colson, T.; Villanova, L.; Buso, D. *Nat. Commun.* **2011**, *2*, 237. (n) Bux, H.; Liang, F.; Li, Y.; Cravillon, J.; Wiebcke, M.; Caro, J. *J. Am. Chem. Soc.* **2009**, *131*, 16000. (o) Venna, S. R.; Carreon, M. A. *J. Am. Chem. Soc.* **2009**, *132*, 76.

(5) (a) Colomban, P. *Chemistry of Solid State Chemistry 2. Proton Conductors*; Cambridge University Press: Cambridge, UK, 1992. (b) Service, R. F. *Science* **2002**, *296*, 1222. (c) Halle, S. M.; Boysen, D. A.; Chisholm, C. R. I.; Merle, R. B. *Nature* **2001**, *410*, 910. (d) Kreuer, K. D. *Chem. Mater.* **1996**, *8*, 610. (e) Kreuer, K. D. *Solid State Ionics* **1997**, *97*, 1.

(6) (a) Akutsu-Sato, A.; Akutsu, H.; Turner, S. S.; Day, P.; Probert, M. R.; Howard, J. A. K.; Akutagawa, T.; Takeda, S.; Nakamura, T.; Mori, T. *Angew. Chem., Int. Ed.* **2005**, *117*, 296. (b) Fujishima, M.; Kanda, S.; Mitani, T.; Kitagawa, H. *Synth. Met.* **2001**, *119*, 485. (c) Nagao, Y.; Ikeda, R.; Kanda, S.; Kubozono, Y.; Kitagawa, H. *Mol. Cryst. Liq. Cryst.* **2002**, *379*, 89. (d) Yamada, T.; Sadakiyo, M.; Kitagawa, H. *J. Am. Chem. Soc.* **2009**, *131*, 3144. (e) Sadakiyo, M.; Yamada, T.; Kitagawa, H. *J. Am. Chem. Soc.* **2009**, *131*, 9906. (f) Morikawa, S.; Yamada, T.; Kitagawa, H. *Chem. Lett.* **2009**, *38*, 654. (g) Bureekaew, S.; Horike, S.; Higuchi, M.; Mizuno, M.; Kawamura, T.; Tanaka, D.; Yanai, N.; Kitagawa, S. *Nat. Mater.* **2009**, *8*, 831. (h) Kanaizuka, K.; Iwakiri, S.; Yamada, T.; Kitagawa, H. *Chem. Lett.* **2010**, *39*, 28. (i) Ōkawa, H.; Sadakiyo, M.; Shigematsu, A.; Miyakawa, T.; Ohba, M.; Kitagawa, H. *J. Am. Chem. Soc.* **2009**, *131*, 13516. (j) Sadakiyo, M.; Ōkawa, H.; Shigematsu, A.; Ohba, M.; Yamada, T.; Kitagawa, H. *J. Am. Chem. Soc.* **2012**, *134*, 5472. (k) Taylor, J. M.; Mah, R. K.; Moudrakovski, I. L.; Ratcliffe, C. I.; Vaidhyanathan, R.; Shimizu, G. K. H. *J. Am. Chem. Soc.* **2010**, *132*, 14055. (l) Horike, S.; Kamitsubo, Y.; Inukai, M.; Fukushima, T.; Umeyama, D.; Itakura, T.; Kitagawa, S. *J. Am. Chem. Soc.* **2013**, *135*, 4612. (m) Taylor, J. M.; Dawson, K. W.; Shimizu, G. K. H. *J. Am. Chem. Soc.* **2013**, *135*, 1193.

(7) Ponomareva, V. G.; Kovalenko, K. A.; Chupakhin, A. P.; Dybtsev, D. N.; Shutova, E. S.; Fedin, V. P. *J. Am. Chem. Soc.* **2012**, *134*, 15640.

(8) (a) Schoenecker, P. M.; Carson, C. G.; Jasuja, H.; Flemming, C. J. J.; Walton, K. S. *Ind. Eng. Chem. Res.* **2012**, *51*, 6513. (b) Küsgens, P.; Rose, M.; Senkovska, I.; Fröde, H.; Henschel, A.; Siegle, S.; Kaskel, S. *Microporous Mesoporous Mater.* **2009**, *120*, 325.

(9) Jeong, N. C.; Samanta, B.; Lee, C. Y.; Farha, O. K.; Hupp, J. T. *J. Am. Chem. Soc.* **2012**, *134*, 51.

(10) Umeyama, D.; Horike, S.; Inukai, M.; Itakura, T.; Kitagawa, S. *J. Am. Chem. Soc.* **2012**, *134*, 12780.